6. J. E. Northrup, *Phys. Rev. Lett.* **57**, 154 (1986).
7. For an analogy with Cl_2/Si(111)-(7×7), see J. J. Boland and J. S. Villarrubia, *Phys. Rev. B* **41**, 9865 (1991).
8. C. J. Wu and E. A. Carter, *J. Am. Chem. Soc.* **113**, 9061 (1991); *Phys. Rev. B* **45**, 9065 (1992).
9. F. R. McFreely, J. F. Morar, N. D. Shinn, G. Landgren, F. J. Himpsel, *Phys. Rev. B* **30**, 764 (1984).
10. A. Szabó, P. D. Farrall, T. Engel, *J. Appl. Phys.* **75**, 3623 (1994).
11. Estimated from the bond strength of the diatomic BrSi.
12. M. Chander, Y. Z. Li, D. Rioux, J. H. Weaver, *Phys. Rev. Lett.* **71**, 4154 (1993); D. Rioux, M. Chander, Y. Z. Li, J. H. Weaver, *Phys. Rev. B* **49**, 11071 (1994).
13. H. Brune *et al.*, *J. Chem. Phys.* **99**, 2128 (1993).
14. We thank E. Carter for insightful discussions. This work was supported by the National Science Foundation (grant DMR 9307259), the Air Force Office of Scientific Research (grant F496209410075), and the Packard Foundation.

9 August 1994; accepted 10 November 1994

Absorption of Solar Radiation by Clouds: Observations Versus Models

R. D. Cess, M. H. Zhang, P. Minnis, L. Corsetti, E. G. Dutton, B. W. Forgan, D. P. Garber, W. L. Gates, J. J. Hack, E. F. Harrison, X. Jing, J. T. Kiehl, C. N. Long, J.-J. Morcrette, G. L. Potter, V. Ramanathan, B. Subasilar, C. H. Whitlock, D. F. Young, Y. Zhou

There has been a long history of unexplained anomalous absorption of solar radiation by clouds. Collocated satellite and surface measurements of solar radiation at five geographically diverse locations showed significant solar absorption by clouds, resulting in about 25 watts per square meter more global-mean absorption by the cloudy atmosphere than predicted by theoretical models. It has often been suggested that tropospheric aerosols could increase cloud absorption. But these aerosols are temporally and spatially heterogeneous, whereas the observed cloud absorption is remarkably invariant with respect to season and location. Although its physical cause is unknown, enhanced cloud absorption substantially alters our understanding of the atmosphere's energy budget.

A companion study herein (*1*) highlights a potential shortcoming in our knowledge of cloud-climate interactions: solar (shortwave) absorption by the cloudy atmosphere is greater than theoretical models predict. This result was based on an analysis of the energy budget of the western Pacific warm pool. Shortwave (SW) cloud forcing (C_s) refers to the difference between cloudy-sky (all-sky) and clear-sky net downward (downward minus upward) SW radiation, either at the top of the atmosphere (TOA) or at the surface. Closure of the energy budget requires that the value for C_s at the surface is 1.5 times greater than that at the TOA. Theoretical cloud radiative transfer models typically produce a ratio near unity (*1*), and for the warm pool this amounts to an underestimate in atmospheric SW absorption by more than 30 W m^{-2}, a substantial discrepancy. This result implies that the clouds absorbed more SW radiation than expected. There has been a long history of unexplained anomalous cloud absorption of uncertain magnitude (*2*).

Here, we describe different measurements that address this problem: collocated satellite (TOA) and surface SW measurements that provide a direct assessment of SW absorption by the cloudy atmosphere. For comparison with the collocated data, we used output from two atmospheric general circulation models (GCMs): the European Centre for Medium-Range Weather Forecasts Model (ECMWF GCM; cycle 36 as used at Lawrence Livermore National Laboratory) and version 2 of the National Center for Atmospheric Research Community Climate Model (CCM2). For both, a Gaussian grid of 2.8° by 2.8° was adopted. Many of the ECMWF GCM results were repeated with a 1.1° by 1.1° grid; no dependence on spatial resolution was noted for this study. Like those in the companion study (*1*), our results show considerable and unexplained cloud SW absorption compared to that in the models.

Satellite-surface measurements were collocated at five different locations (Table 1). At Boulder, Colorado, near-surface measurements were made from upward- and downward-facing pyranometers mounted at the top of the 300-m National Oceanic and Atmospheric Administration (NOAA) Boulder Atmospheric Observatory (BAO) tower, thus providing values for the net downward SW. Two sets of collocated satellite data were used. One (Boulder ERBS) consisted of net downward SW at the TOA as measured by the Earth Radiation Budget Experiment (ERBE) SW scanner on the Earth Radiation Budget Satellite (ERBS), whose orbit has a 57° inclination to the equator and provides a sampling of each local hour angle every 36 days. To avoid the foothills of the Rocky Mountains, we ensured that all measurements were averages of pixels falling within a grid extending 0.3°N, 0.3°S, and 0.7°E of the tower (*3*). The second Boulder data set (Boulder GOES), and that for the Wisconsin pyranometer network, used TOA broadband (0.2- to 5.0-μm) albedos computed with the use of visible channel (0.55 to 0.75 μm) brightness counts from the Geostationary Operational Environmental Satellite (GOES) centered over the BAO tower and over each of the individual pyranometer locations of the Wisconsin network (*4*).

The other sites (including Wisconsin) had only upward-facing pyranometers and so provided data on surface insolation (downward SW) rather than for net downward SW at the surface. The collocations of ERBE pixel data at Barrow, Cape Grim, and American Samoa were similar to those in Boulder, except that pixels were averaged over 1° by 1° grids centered at the pyranometer locations. Because ERBS did not view Barrow, ERBE measurements from NOAA 9 (July 1985 and 1986) and NOAA 10 (July 1987) were used. These satellites had sun-synchronous orbits with equator crossing times of 1430 local time (LT) (NOAA 9) and 0730 LT (NOAA 10). Because of its high latitude, Barrow was viewed several times a day by each satellite. The surface measurements were subject to errors typically associated with commercial pyranometers. But several factors resulted in significant error reductions (*5*), so that the accuracy of the surface measurements was limited primarily by the linearity of the instruments, which is better than about 0.5%.

R. D. Cess, M. H. Zhang, X. Jing, Y. Zhou, Institute for Terrestrial and Planetary Atmospheres, Marine Sciences Research Center, State University of New York, Stony Brook, NY 11794, USA.
P. Minnis, E. F. Harrison, C. H. Whitlock, Atmospheric Sciences Division, NASA Langley Research Center, Hampton, VA 23665, USA.
L. Corsetti, W. L. Gates, G. L. Potter, Program for Climate Model Diagnosis and Intercomparison, Lawrence Livermore National Laboratory, Livermore, CA 94550, USA.
E. G. Dutton, Climate Monitoring and Diagnostics Laboratory, Environmental Research Laboratories–National Oceanic and Atmospheric Association, Boulder, CO 80303, USA.
B. W. Forgan, Bureau of Meteorology, G.P.O. Box 1298K, Melbourne, 3001 Victoria, Australia.
D. P. Garber and D. F. Young, Lockheed Engineering and Science Company, Hampton, VA 23666, USA.
J. J. Hack and J. T. Kiehl, National Center for Atmospheric Research, Boulder, CO 80307, USA.
C. N. Long, Department of Meteorology, Pennsylvania State University, University Park, PA 16802, USA.
J.-J. Morcrette, European Centre for Medium-Range Weather Forecasts, Reading, Berkshire RG29AX, UK.
V. Ramanathan and B. Subasilar, Center for Clouds, Chemistry and Climate, Scripps Institution of Oceanography, University of California at San Diego, La Jolla, CA 92126, USA.

The Boulder GOES data set demonstrated two points. First, it produced a surface-to-TOA cloud forcing ratio that was near 1.5, as did the Pacific warm pool analysis (*1*); second, this result was consistent with an alternate interpretation using surface insolation. We first consider the cloud forcing ratio. Evaluation of surface and TOA cloud forcing, $C_s(S)$ and $C_s(TOA)$, respectively, required identification of clear-sky measurements that for a given solar zenith angle correspond to the maximum values of net downward SW at both the TOA and the surface. These are represented by linear fits (3) in Fig. 1. The difference between each measurement and the clear-sky fit provided values for C_s for each measurement. The dayside means were $C_s(S) = -92.6$ W m^{-2} and $C_s(TOA) = -63.2$ W m^{-2}, or $C_s(S)/C_s(TOA) = 1.46$, virtually identical to the values obtained in the warm pool analysis (*1*). Because theoretical models typically yield a value for the ratio of $C_s(S)/C_s(TOA)$ of ≈ 1, the observed value of 1.46 means that the cloudy atmosphere is absorbing roughly 30 W m^{-2} more SW radiation than expected, which here is the difference between $C_s(TOA)$ and $C_s(S)$.

This analysis, however, has two drawbacks. First, only surface insolation, rather than net downward SW at the surface, was available at the other sites. Second, an unambiguous clear-sky identification at the surface, using the linear-fit approach (Fig. 1B), was not applicable at some other sites. This was because of a common phenomenon in which broken clouds that do not shadow a pyranometer can actually supply diffuse radiation to it, so that the surface insolation can exceed that for clear skies. This broken cloud effect was pronounced in the data for Wisconsin and for American Samoa in late 1986 and throughout 1987 (during El Niño), as was evident from scatter plots similar to Fig. 1B.

We therefore used an alternate approach patterned after a study of Antarctic clouds

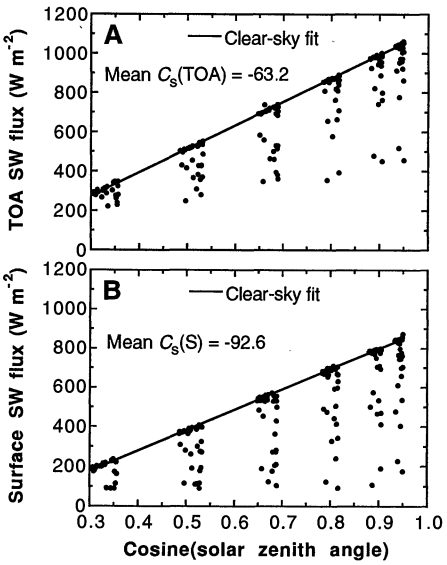

Fig. 1. (**A**) The net downward SW flux at the TOA, as measured by GOES at the BAO tower, as a function of the cosine of the solar zenith angle. (**B**) The same as (A) but for the tower-measured net downward SW flux at the surface.

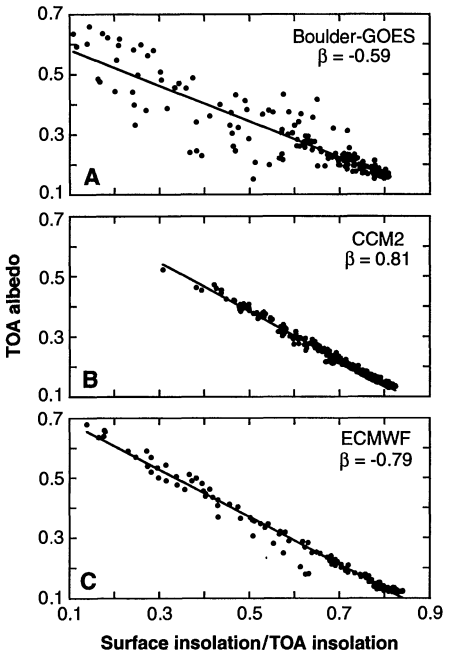

Fig. 2. (**A**) Scatter plot of the GOES TOA albedo as a function of surface insolation (measured at the BAO tower) divided by the TOA insolation. (**B**) The same as (A) but for CCM2. (**C**) The same as (A) but for the ECMWF GCM. In (A) through (C), the solid line represents a linear root mean square fit.

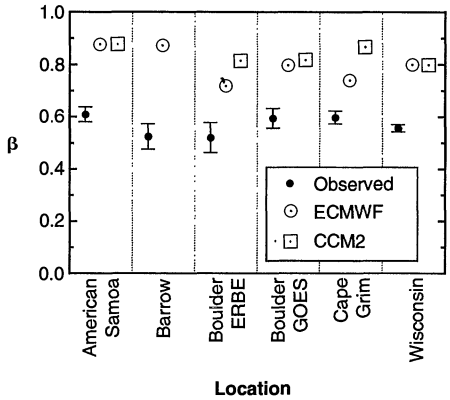

Fig. 3. Comparison of values of β (determined from the ECMWF GCM and CCM2) with the observed values. The vertical bars denote the 95% confidence intervals of the observations.

Table 1. Summary of collocated satellite-surface measurements used in our study; all refer to broad-band (0.2- to 5.0-μm) SW fluxes. Blank spaces indicate instantaneous ERBS measurements temporally collocated within the hour bin (American Samoa and Boulder) or half-hour bin (Cape Grim) of the pyranometer measurements.

Location	Time period	Satellite-pyranometer collocation	Measurements (*n*)
American Samoa* 14.25°S and 170.56°W	3 years: 1985 to 1987		934
Barrow* 71.32°N and 157°W	3 months: July 1985, 1986, and 1987	Instantaneous NOAA 9 and 10 measurements temporally collocated within the hour bin of pyranometer measurements.	223
Boulder* 40.05°N and 105.01°W	7 months: April through September 1986 and July 1987		239
Boulder* 40.05°N and 105.01°W	21 days: 29 June 1987 to 19 July 1987	Hourly means from three consecutive half-hour GOES measurements temporally collocated with hourly mean pyranometer measurements.	202
Cape Grim 40.68°S and 144.69°E	3 years: 1985 to 1987		1419
Wisconsin (see Fig. 5A)	22 days: 12 October 1986 to 2 November 1986	Instantaneous GOES measurements temporally collocated within the minute bin of individual pyranometers comprising a network of 11 pyranometers.	1914

*NOAA–Climate Monitoring and Diagnostics Laboratory sites.

(6), which refers to the derivative (β) as

$$-\frac{d(\text{TOA albedo})}{d[(\text{surface insolation})/(\text{TOA insolation})]} \quad (1)$$

as evaluated from a linear regression. In Fig. 2, clear skies correspond to points on the right (low TOA albedo and high surface insolation); points progressing to the left indicate increasing cloudiness. Although the results given by the ECMWF GCM exhibited greater cloud variability than did those given by CCM2 (compare Fig. 2C to Fig. 2B), they both produced virtually identical values for β, which indicates that β was not affected by each model's differences in cloud variability nor was dependent on cloud optical depth (including amount and height), as we confirmed through sensitivity studies with CCM2. An increase in SW absorption in a GCM's clouds would be the only way the value for β could be modified to agree with the observed value for β of 0.59. This would simultaneously increase the cloud-induced changes of surface insolation (because less radiation would be transmitted through the clouds while clear skies are unaffected) and would decrease changes in the TOA albedo (because the clouds are darker). Both act to reduce the value of β.

Like $C_s(S)/C_s(TOA)$, β is a direct determinant of cloud absorption. To relate the two, integration of Eq. 1 (using clear skies as a boundary condition) yields

$$C_s(S)/C_s(TOA) = (1-\alpha_s)/\beta \quad (2)$$

where α_s is the surface albedo. This equation applies in the absence of broken-cloud enhancements of surface insolation, as was the case for the Boulder GOES data. From the upward- and downward-facing pyranometer measurements, α_s = 0.17 for the surface under the BAO tower, whereas β = 0.59 (Fig. 2A). Thus, $C_s(S)/C_s(TOA)$ = 1.41, in agreement with the value of 1.46 from Fig. 1, whereas for the two GCMs, $C_s(S)/C_s(TOA)$ = 1.07. Thus, both interpretations demonstrate that the GCMs underestimate cloud absorption; the advantage of β is that it uses surface insolation.

At all locations, the two GCMs significantly overestimated β (Fig. 3) and thus underestimated cloud SW absorption. There was a remarkable geographical invariance of the observed values for β, but there could be exceptions. An increase in surface albedo will increase the clear-sky TOA albedo more than that for overcast conditions, thereby reducing β. As an example, a collocated South Pole data set (6), where the surface albedo was 0.81, produced a value for β of roughly half the magnitude of those values shown in Fig. 3. It is for this reason that we do not show CCM2 results for Barrow in Fig. 3. This model was in agreement with the observed Barrow value because it incorrectly prescribed snow and ice in the Barrow grid for July, and the high surface albedo resulted in a spurious reduction in the model's value for β. The example of the South Pole, representing an extreme increase in surface albedo, suggests there should be little difference in values for β for ocean and vegetated surfaces because of the relatively small differences in surface albedo, consistent with Fig. 3.

Clear skies are drier than when clouds are present. Thus, in progressing to the left in Fig. 2A there would be a related increase in column water vapor that might explain our observations of β—that is, increased atmospheric absorption could be caused by increased water vapor associated with clouds rather than by the clouds themselves. To demonstrate that this is not the case, we performed a two-variable regression, in contrast to the one-variable regression of Fig. 2A, with ECMWF column water vapor (7) as the second variable. For the two-variable regression, β is defined by Eq. 1 as a partial derivative. For all data sets, the two separate regressions produced virtually identical β values.

The Cape Grim and American Samoa data exhibited interannual variability; the most extreme data were from American Samoa, for which the annual mean surface insolation in 1987 (when broken cloud effects were apparent in the data) was 11% greater than that for 1985. But the values for β exhibited little interannual variability (Fig. 4A), which emphasized that they were a measure of cloud absorption and not cloud geometry. Seasonal dependency was likewise minimal (Fig. 4B).

We compared here single GCM grid points to point (pyranometer) measurements; whether either is representative of larger regions is unknown. If they are representative, then the point measurements should be representative of the 2.8° by 2.8° GCM grids. For the GCMs, it was easily demonstrated that values for β at specific grid points were representative of larger regions comprising adjacent grid points. The Wisconsin pyranometer network provided the same conclusion with respect to point measurements. Virtually the same value for β was obtained for each of the individual collocated data sets (or point measurements), as shown in Fig. 5. This result, combined with the results in Fig. 3, demonstrated that values for β were remarkably invariant with respect to geographical location on all spatial scales. The only exceptions were found for regions with high surface albedos.

Our results, and those of others (*1*), point to a shortcoming in our knowledge of cloud radiative transfer processes. There is no obvious explanation for the cause of the enhanced cloud SW absorption. Increased cloud SW absorption resulting from aerosol

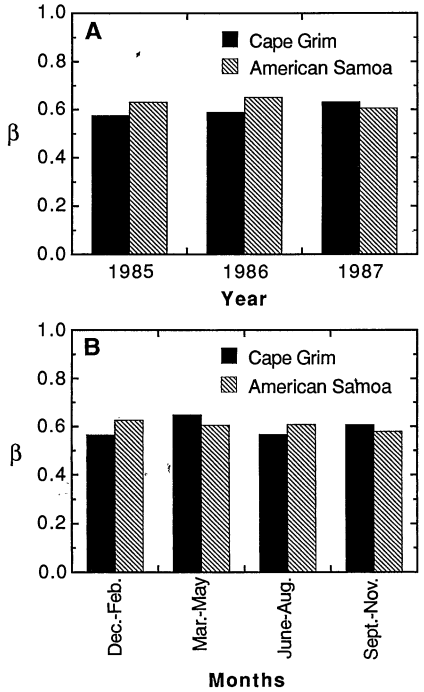

Fig. 4. (**A**) Interannual variability of β for Cape Grim and American Samoa. (**B**) Seasonal variability of β for Cape Grim and American Samoa computed from 3-year composites.

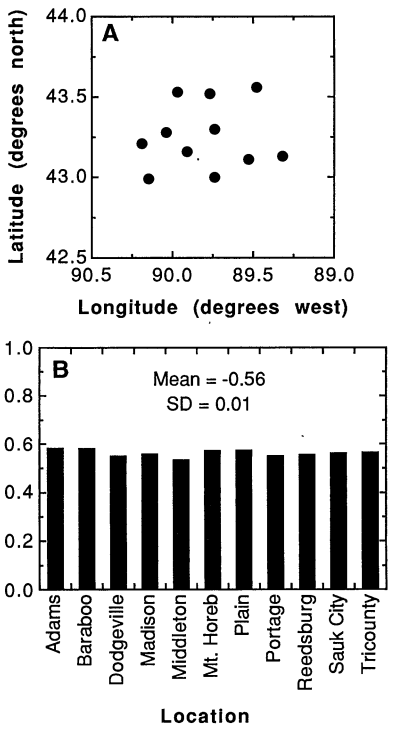

Fig. 5. (**A**) Pyranometer locations for the Wisconsin site. (**B**) Values for β as determined from collocated GOES pyranometer measurements at each pyranometer location in Wisconsin.

effects has been studied for at least 25 years (*2*). An aerosol influence on cloud albedo should show temporal and spatial variability because of the heterogeneous nature of tropospheric aerosols. But there was little interannual or seasonal variability in values of β for Cape Grim and American Samoa (Fig. 4) nor was there significant geographic variability (Fig. 3). If aerosol effects were important in determining β, these variations should be much larger. Cape Grim in particular is known to be a fairly clean site with regard to aerosols; the boundary layer concentration of cloud nuclei is largest in the period from December through February (*8*), and the aerosol optical depth at visible wavelengths peaks in the period from September through November (*9*). But values of β for these periods differ little from those obtained in March through May and June through August (Fig. 4B).

Although only two GCMs were used in this comparison between models and observations, comparable discrepancies have been reported for more detailed cloud radiative transfer models than typically used in GCMs (*1*). These studies also investigated the role of cloud interstitial water vapor and showed that this was not the cause of the enhanced absorption. The enhanced cloud SW absorption phenomenon is of significant magnitude. Averaged over the globe and annually, $C_s(TOA) \approx -50$ W m^{-2} (*10*), whereas the average observed value for β is 0.55 versus 0.80 for the GCMs (Fig. 3). For a global mean surface albedo of 0.1, Eq. 2 indicates that enhanced cloud SW absorption, by itself, should reduce global mean SW surface absorption by about 25 W m^{-2} relative to contemporary climate models. This significant discrepancy is consistent with a comparison of four GCMs to surface measurements (*11*) in which cloud effects were not isolated and the TOA SW flux was not constrained. Our finding of enhanced cloud SW absorption is also consistent with an earlier satellite-surface measurement study restricted to the eastern United States (*12*).

REFERENCES AND NOTES

1. V. Ramanathan *et al.*, *Science* **267**, 499 (1995).
2. G. L. Stephens and S.-C. Tsay, *Q. J. R. Meteorol. Soc.* **116**, 671 (1990); I. N. Mel'nikova and V. V. Mikhaylov, *J. Atmos. Sci.* **51**, 925 (1994).
3. R. D. Cess *et al.*, *J. Climate* **6**, 308 (1993).
4. For the BAO tower, average TOA reflectances were computed for 12 by 12 arrays of half-hourly GOES-West 1-km pixels as described (*13*) and converted to narrow-band albedos with the use of the ERBE anisotropic reflectance model (*14*), which varies with the degree of cloudiness. The same technique was applied to 8 by 8 arrays of hourly GOES-East 1-km pixels over each of the Wisconsin pyranometer locations (*15*) with the use of the conversion from brightness counts to reflectance (*16*). Narrow-band albedos were then converted to broad-band albedos for both locations (*17*).
5. The data were taken at sites where extensive attention was given to ongoing calibration and operational accuracy. Also, calibration errors and residual long-term drifts were eliminated through the regression analyses, as was also the case for the satellite measurements.
6. S. Nemesure *et al.*, *J. Climate* **7**, 579 (1994).
7. K. E. Trenberth, *NCAR TN-73+STR* (National Center for Atmospheric Research, Boulder, CO, 1992).
8. J. L. Gras, *J. Atmos. Chem.* **11**, 89 (1989).
9. B. W. Forgan and P. J. Fraser, *Baseline Atmospheric Program (Australia) 1985* (Australian Bureau of Meteorology, Melbourne, 1987).
10. E. F. Harrison *et al.*, *J. Geophys. Res.* **95**, 18687 (1990).
11. J. R. Garratt, *J. Climate* **7**, 72 (1994).
12. C. G. Justus, *Proceedings of the Conference on Satellite Meteorology/Remote Sensing Applications* (American Meteorological Society, Boston, MA, 1984), p. 197.
13. P. Minnis *et al.*, *J. Appl. Meteorol.* **31**, 317 (1992).
14. J. T. Suttles *et al.*, "Angular radiation models for Earth-atmosphere system," *NASA RP-1184* (1988), shortwave radiation, vol. 1.
15. C. H. Whitlock *et al.*, *NASA TM 100485* (1987); C. H. Whitlock *et al.*, *NASA TM 102596* (1990). Of the 17 pyranometers, we used only those 11 that provided continuous measurements throughout the measurement period, which started at noon LT on 12 October 1986 and extended through 2 November 1986.
16. P. Minnis, P. W. Heck, D. F. Young, *J. Atmos. Sci.* **50**, 1305 (1993).
17. The broad-band albedo (α_B) was estimated from the narrow-band albedo (α_N) through

$$\alpha_B = a_0 + a_1\alpha_N + a_2\alpha_N^2 + a_3 \ln(\sec \theta_0)$$

where θ_0 is the solar zenith angle. For the BAO tower location, the coefficients a_i were determined through multiple regression with the use of 2.5° by 2.5° ERBS and NOAA 9 ERBE-scanner instantaneous albedos and matched to 2.5° by 2.5° GOES narrow-band albedos. To ensure that background and atmospheric conditions were similar to those in the vicinity of the BAO tower, we took regression data between 100°W and 105°W and 35°N to 45°N, during the same period as the Boulder GOES-data. A similar procedure, using ERBS, was applied to the Wisconsin sites, with the regression coefficients based on 2.5° by 2.5° data between 90°W and 100°W and 35°N to 45°N, during October 1986.

18. This research was supported by Department of Energy (DOE) grants DEFG0285ER60314 and DEFG0290ER61063 and NASA grants NAG11264 and NAGW3517 to the State University of New York at Stony Brook; by DOE grant DEFG0593ER61376 to the National Center for Atmospheric Research, which is sponsored by NSF; by the NOAA Climate Monitoring and Diagnostics Laboratory; by NSF grants ATM 8920119 and ATM 9011259 to the Scripps Institution of Oceanography; and by DOE contract W-7405-ENG-48 to Lawrence Livermore National Laboratory. The ECMWF's permission to use their GCM in this study is gratefully acknowledged.

24 August 1994; accepted 14 November 1994

Warm Pool Heat Budget and Shortwave Cloud Forcing: A Missing Physics?

V. Ramanathan,* B. Subasilar, G. J. Zhang, W. Conant, R. D. Cess, J. T. Kiehl, H. Grassl, L. Shi

Ship observations and ocean models indicate that heat export from the mixed layer of the western Pacific warm pool is small (<20 watts per square meter). This value was used to deduce the effect of clouds on the net solar radiation at the sea surface. The inferred magnitude of this shortwave cloud forcing was large (≈−100 watts per square meter) and exceeded its observed value at the top of the atmosphere by a factor of about 1.5. This result implies that clouds (at least over the warm pool) reduce net solar radiation at the sea surface not only by reflecting a significant amount back to space, but also by trapping a large amount in the cloudy atmosphere, an inference that is at variance with most model results. The excess cloud absorption, if confirmed, has many climatic implications, including a significant reduction in the required tropics to extratropics heat transport in the oceans.

What effect do clouds have on the atmospheric solar absorption? This question is fundamental to the issue of how clouds influence climate and climate change. Clouds reduce the solar radiation absorbed by the surface-atmosphere system—that is, the shortwave (SW) cloud forcing at the top of the atmosphere [$C_s(TOA)$] is less than 0. The global annual mean value for $C_s(TOA)$ (*1*) is about −45 to −50 W m^{-2}. This value is negative because clouds in general reflect more solar radiation back to space than a cloudless atmosphere. $C_s(TOA)$ can be partitioned in terms of $C_s(S)$, the effect of clouds on the surface, and of $C_s(A)$, the effect on the atmospheric column. If clouds enhance the solar absorption by the atmospheric column when compared to the solar absorption with a clear-sky atmosphere, then $C_s(A) > 0$. Here, we used measurements of oceanic heat transport and of the surface heat budget in the warm western Pacific ocean to deduce values for $C_s(A)$. A companion

V. Ramanathan, B. Subasilar, G. J. Zhang, W. Conant, Center for Clouds, Chemistry and Climate, Scripps Institution of Oceanography, University of California at San Diego, La Jolla, CA 92093, USA.
R. D. Cess, Institute for Terrestrial and Planetary Atmospheres, Marine Science Research Center, State University of New York, Stony Brook, NY 11794, USA.
J. T. Kiehl, National Center for Atmospheric Research, Boulder, CO 80307, USA.
H. Grassl, Max-Planck-Institut Fur Meteorologie, Bundesstraße 55, D-020146 Hamburg, Germany.
L. Shi, SeaSpace Corporation, San Diego, CA 92126, USA.

*To whom correspondence should be addressed.